

SANDIA REPORT

SAND2021-11708

Printed September 2021



Sandia
National
Laboratories

Locating Seismic Events with Local-Distance Data

Kathy Davenport

Prepared by
Sandia National Laboratories
Albuquerque, New Mexico
87185 and Livermore,
California 94550

Issued by Sandia National Laboratories, operated for the United States Department of Energy by National Technology & Engineering Solutions of Sandia, LLC.

NOTICE: This report was prepared as an account of work sponsored by an agency of the United States Government. Neither the United States Government, nor any agency thereof, nor any of their employees, nor any of their contractors, subcontractors, or their employees, make any warranty, express or implied, or assume any legal liability or responsibility for the accuracy, completeness, or usefulness of any information, apparatus, product, or process disclosed, or represent that its use would not infringe privately owned rights. Reference herein to any specific commercial product, process, or service by trade name, trademark, manufacturer, or otherwise, does not necessarily constitute or imply its endorsement, recommendation, or favoring by the United States Government, any agency thereof, or any of their contractors or subcontractors. The views and opinions expressed herein do not necessarily state or reflect those of the United States Government, any agency thereof, or any of their contractors.

Printed in the United States of America. This report has been reproduced directly from the best available copy.

Available to DOE and DOE contractors from

U.S. Department of Energy
Office of Scientific and Technical Information
P.O. Box 62
Oak Ridge, TN 37831

Telephone: (865) 576-8401
Facsimile: (865) 576-5728
E-Mail: reports@osti.gov
Online ordering: <http://www.osti.gov/scitech>

Available to the public from

U.S. Department of Commerce
National Technical Information Service
5301 Shawnee Rd
Alexandria, VA 22312

Telephone: (800) 553-6847
Facsimile: (703) 605-6900
E-Mail: orders@ntis.gov
Online order: <https://classic.ntis.gov/help/order-methods/>



ABSTRACT

As the seismic monitoring community advances toward detecting, identifying, and locating ever-smaller natural and anthropogenic events, the need is constantly increasing for higher resolution, higher fidelity data, models, and methods for accurately characterizing events. Local-distance seismic data provide robust constraints on event locations, but also introduce complexity due to the significant geologic heterogeneity of the Earth's crust and upper mantle, and the relative sparsity of data that often occurs with small events recorded on regional seismic networks. Identifying the critical characteristics for improving local-scale event locations and the factors that impact location accuracy and reliability is an ongoing challenge for the seismic community. Using Utah as a test case, we examine three data sets of varying duration, finesse, and magnitude to investigate the effects of local earth structure and modeling parameters on local-distance event location precision and accuracy. We observe that the most critical elements controlling relocation precision are azimuthal coverage and local-scale velocity structure, with tradeoffs based on event depth, type, location, and range.

This page left blank.

CONTENTS

1.	Background.....	9
1.1.	Challenges.....	9
2.	Software and models.....	10
2.1.	GeoTess software used in event locations	11
2.1.1.	LocOO3D	11
2.1.2.	GeoTess	11
2.1.3.	PCalc.....	11
2.1.4.	Bender	12
2.2.	Velocity Models	12
2.3.	Seismicity Depth Model	14
3.	Event Relocations.....	15
3.1.	Data	15
3.1.1.	UUSS Catalog.....	15
3.1.2.	UUEB Catalog	16
3.1.3.	Redmond Salt Mine Catalog	17
3.2.	Event Relocations	18
3.2.1.	Events from the UUSS Catalog	18
3.2.2.	Events from the UUEB Catalog.....	22
3.2.3.	Events from the Redmond Catalog.....	24
4.	Summary	26

LIST OF FIGURES

Figure 1.	Velocity models for the crust. Top: Upper-crust P-wave velocity in the SALSA3Dv2 (left) and SALSA3Dv3 (right) models. Middle: Mid-crust P-wave velocity in the SALSA3Dv2 and SALSA3Dv3 models. Bottom: P-wave velocities at 10, 20, and	13
Figure 2.	Seismicity Depth Model. Top: Upper limit of the allowable seismicity depth based on topography from ETOPO1. Inset: High-resolution seismicity depth limit based on topography in Utah. Bottom: Lower limit of the allowable seismicity depth based on historic seismic activity and known tectonics.....	14
Figure 3.	UUSS seismic catalog information. Left: Map showing seismic stations (purple triangles) included in the data in the UUSS catalog. White dot shows location of Bingham Mine ground truth events. Right (top to bottom): Distribution of events based on event type. Distribution of arrivals based on phase identification. Arrival times as a function of distance.....	15
Figure 4.	UUEB seismic catalog information. Left: Map showing seismic stations (purple triangles) included in the UUSS catalog data. Right (top to bottom): Distribution of events based on event type. Distribution of arrivals based on phase identification. Arrival times as a function of distance.....	16
Figure 5.	Redmond Salt Mine seismic catalog information. Left: Map showing seismic stations (purple triangles) included in the Redmond catalog data. Right (top to bottom): Distribution of events based on event type. Distribution of arrivals based on phase identification. Arrival times as a function of distance	17
Figure 6.	Data distribution for each catalog. Arrivals plotted by number of stations and maximum azimuthal gap. Clockwise from left: UUSS catalog, UUEB catalog, Redmond catalog.....	18

Figure 7. Distance between UUSS Catalog event locations and relocated sources. Based on travel time predictions using velocity models (clockwise from top left) AK135, IASP91, RSTT, Utah3D, SALSA3Dv3, and SALSA3Dv2. Symbol color and size represent distance between catalog origin and relocated source location for each velocity model.....	19
Figure 8. Mean distances between event origins. Left: Mean distances by velocity model. White diamonds represent mean, color bars represent range of 25th and 75th percentiles, black dots represent outliers. Top chart is locations relative to the UUSS catalog locations. Bottom chart is locations relative to AK135 locations. Right: Distance between locations as a function of the number of stations with time-defining arrivals, and distance between locations as a function of azimuthal gap at the origin location.....	20
Figure 9. 95% Confidence ellipses based on maximum azimuthal gap. Left: Events with a maximum azimuthal gap < 180 degrees. Right: Events with maximum azimuthal gap > 180 degrees.....	20
Figure 10. Distance between locations based on initial origins from the UUSS catalog and AK135 locations.....	21
Figure 11. Differences between locations based on initial origin location. Left: Mean distance between locations based on UUSS catalog and AK135 starting origin locations by velocity model. Right: Location differences based on azimuthal gap and total number of location differences.....	21
Figure 12. Distance between UUEB Catalog event locations and relocated sources. Based on travel time predictions using velocity models (clockwise from top left) AK135, IASP91, RSTT, Utah3D, SALSA3Dv3, and SALSA3Dv2. Symbol color and size represent distance between catalog origin and relocated source location for each velocity model.....	22
Figure 13. Mean distances between event origins. Left: Mean distances by velocity model. White diamonds represent mean, color bars represent range of 25th and 75th percentiles, black dots represent outliers. Top chart is locations relative to the UUEB catalog locations. Bottom chart is locations relative to AK135 locations. Right: Distance between locations as a function of the number of stations with time-defining arrivals, and distance between locations as a function of azimuthal gap at the origin location.....	23
Figure 14. Distance between Redmond Catalog event locations and relocated sources. Based on travel time predictions using velocity models (clockwise from top left) AK135, IASP91, RSTT, Utah3D, SALSA3Dv3, and SALSA3Dv2. Symbol color and size represent distance between catalog origin and relocated source location for each velocity model.....	24
Figure 15. Mean distances between event origins. Left: Mean distances by velocity model. White diamonds represent mean, color bars represent range of 25th and 75th percentiles, black dots represent outliers. Top chart is locations relative to the Redmond catalog locations. Bottom chart is locations relative to AK135 locations. Right: Distance between locations as a function of the number of stations with time-defining arrivals, and distance between locations as a function of azimuthal gap at the origin location.....	25

This page left blank

ACRONYMS AND DEFINITIONS

Abbreviation	Definition
CSS	Center for seismic studies
1D	One-dimensional
3D	Three-dimensional
SALSA3D	Sandia Los Alamos 3D model
RSTT	Regional seismic travel time
UUEB	Unconstrained Utah event bulletin
UUSS	University of Utah seismograph stations

1. BACKGROUND

Locating and characterizing seismic events is a foundational task of the seismic monitoring community. As we move toward detecting, identifying, and locating ever-smaller natural and anthropogenic events, local-scale data become increasingly significant as fewer stations reliably record lower magnitude events. Local distance data provide robust constraints on event locations, but also introduce additional complexities due to the significant geologic heterogeneity of the crust and upper mantle and the relative sparsity of data that often occurs with small events recorded on global and regional seismic networks. Identifying the critical characteristics for improving local-scale event locations and the factors that impact location accuracy and reliability is an ongoing challenge for the seismic community.

The work presented here examines events in Utah, which serves as a test location for examining the reliability of event locations based on local-distance seismic phase arrivals. The region is well-instrumented and there is an abundance of data at a range of magnitude scales for both local earthquakes and mining-related explosive events. The larger Utah events include associated phase arrivals that extend to near-regional distances (up to ~ 450 km) and transition from a dominantly crustal-phase regime into mantle-dominated regional distances.

1.1. Challenges

There are numerous practical and technical challenges associated with using local-distance seismic data for locating small magnitude events. Data limitations include a sparsity of station coverage, including often poor azimuthal distribution, and low signal amplitude. Published catalogs often only identify the first body wave arrival as “P”, which is insufficient for predicting appropriate crustal phase (Pg) or upper-most mantle phase (Pn) travel times at local distances. Additionally, local phases are notoriously difficult to approximate with ray theory and often result in travel time predictions that are too fast, particularly beyond cross-over distances ($>\sim 160$ -180 km in average continental crust). Complex crustal velocity structure makes accurate travel time predictions challenging due to resolution limitations for generating and interrogating three-dimensional velocity models.

One of the biggest challenges for locating seismic events with local-scale data involves estimating source depth. Depth is an important discriminant for characterizing source mechanism, yet it is very difficult to estimate based on direct or refracted body wave arrivals. Depth estimates are highly dependent on the accuracy and resolution of the velocity model used for travel time predictions. Events with good station coverage that are located with an inaccurate velocity model may “slingshot” up and down without converging to a good depth estimate due to travel time prediction errors. For this reason, event locations often include a significant error range on depth, even if the lateral location is well constrained, and improving depth estimates is an important consideration for improving local-scale event locations.

This page left blank.

2. SOFTWARE AND MODELS

The broader research topic of improving event locations relies on tools including and beyond location determination algorithms. Current event location work covered in this report predominantly uses the in-house GeoTess suite of software packages, which are publicly available through GitHub. GeoTess packages used in this work are described below.

2.1. GeoTess software used in event locations

2.1.1. LocOO3D

LocOO3D (Object-Oriented 3-Dimensional Location Software) is the software package for determining event locations/relocations based on the travel time prediction method described in Ballard et al. (2009). The algorithm utilizes Levenberg-Marquardt damping (Levenberg, 1944; Marquardt, 1963; Press et al., 2002) within an iterative linear least squares inversion framework (Geiger, 1910; Jordan and Sverdrup, 1981; Lay and Wallace, 1995) to improve event location solutions, particularly for poorly constrained events that violate inherent linearity assumptions. The advantage of the Levenberg-Marquardt transformation as implemented in LocOO3D is that the change in location at each iteration is rotated in the direction of steepest descent in model parameter space, which effectively controls the step direction and magnitude and prevents divergence when a linearized solution alone would fail. Details of the location algorithm, damping, and convergence criteria can be found in the documentation in the LocOO3D GitHub repository.

Important features of LocOO3D include the capability for determining locations using a variety of input velocity models and formats, the ability to include observed arrival time, back-azimuth and horizontal slowness in location calculations, working directly with the CSS3.0 data format (Anderson et al., 1990) commonly used in the seismic monitoring community, reading data from text files or an Oracle database, locating events individually or relative to a master event, and producing sophisticated error estimations including distance dependent uncertainty. The LocOO3D software, documentation, and examples are available at <https://github.com/sandialabs/LocOO3D>.

2.1.2. GeoTess

GeoTess is a 3D model parameterization framework and software system for the construction and interrogation of multi-dimensional Earth models. GeoTess utilizes a tessellation of variably spaced 1D arrays to store a variety of model attributes onto a common grid. 3D velocity models used by LocOO3D for event locations are stored as GeoTess formatted files. The GeoTess framework is described in Ballard et al. (2016) and the software is available at <https://github.com/sandialabs/GeoTessJava>.

2.1.3. PCalc

PCalc is a travel time prediction calculator that allows modeling ray path geometry approximations based on the Bender ray tracer, as used in LocOO3D location calculations. PCalc can compute travel times and ray paths through any Earth velocity model that can be represented using the GeoTess format, and can be used to build 3D travel time correction surfaces for use with LocOO3D. PCalc is available at <https://github.com/sandialabs/PCalc>.

2.1.4. Bender

Bender is the ray tracing utility used by LocOO3D, PCalc, and other GeoTess software for calculating on-the-fly travel times through 3D geotess-formatted velocity models. Bender utilizes a pseudo-bending algorithm based on Um and Thurber (1987) and Zhao et al. (1992) to efficiently predict travel times through a 3D model with an improved ability to satisfy Snell's law at velocity discontinuities and avoid local minima. Bender is included in LocOO3D and PCalc, and is described in detail in Ballard et al. (2009).

2.2. Velocity Models

A reasonable representation of the Earth's seismic velocity structure is a vital component for determining event locations using seismic phase arrival times. While many seismic velocity models ranging from multi-degree global models to meter-scale basin models are available from the geophysical research community, models built to illuminate geologic structure are not always suitable for forward calculating predicted seismic phase travel times. It has been shown that ray tracing methods are not interchangeable for seismic velocity models, so utilizing community models for travel time predictions would require additional constraints to account for path estimation errors. Larger scale models focused on the mantle or whole Earth may be useful for predicting travel times for regional or teleseismic event locations, however they often lack crustal-scale resolution and so do not significantly improve the accuracy of local distance event locations compared to 1D velocity models. For these reasons, this effort focused on relocating events using community-standard 1D velocity models and higher-dimensional models designed for travel time prediction (Figure 1).

The event locations discussed here were determined from local-distance seismic body wave arrival times in and around Utah. Velocity models used for relocations include:

- AK135 1D velocity model (Kennett et al., 1995). Default velocity model for LocOO3D.
- IASP91 1D velocity model (Kennett, 1991)
- Regional Seismic Travel Time (RSTT) (www.sandia.gov/rstt, Phillips et al., 2007)
- SALSA3D Version 2 - 3D tomographic velocity model (Ballard et al., 2016b). Crust2.0 (Bassin et al., 2000) above Moho depths. This is the current stable release of the SALSA3D velocity model.
- SALSA3D Version 3 (beta version) - 3D tomographic velocity model. Crust1.0 (Laske et al., 2013) above Moho depths.
- SALSA3D-Utah (alpha version) - 3D tomographic crustal model across the Wasatch Front Relocation results are compared to the initial catalog locations for each data set.

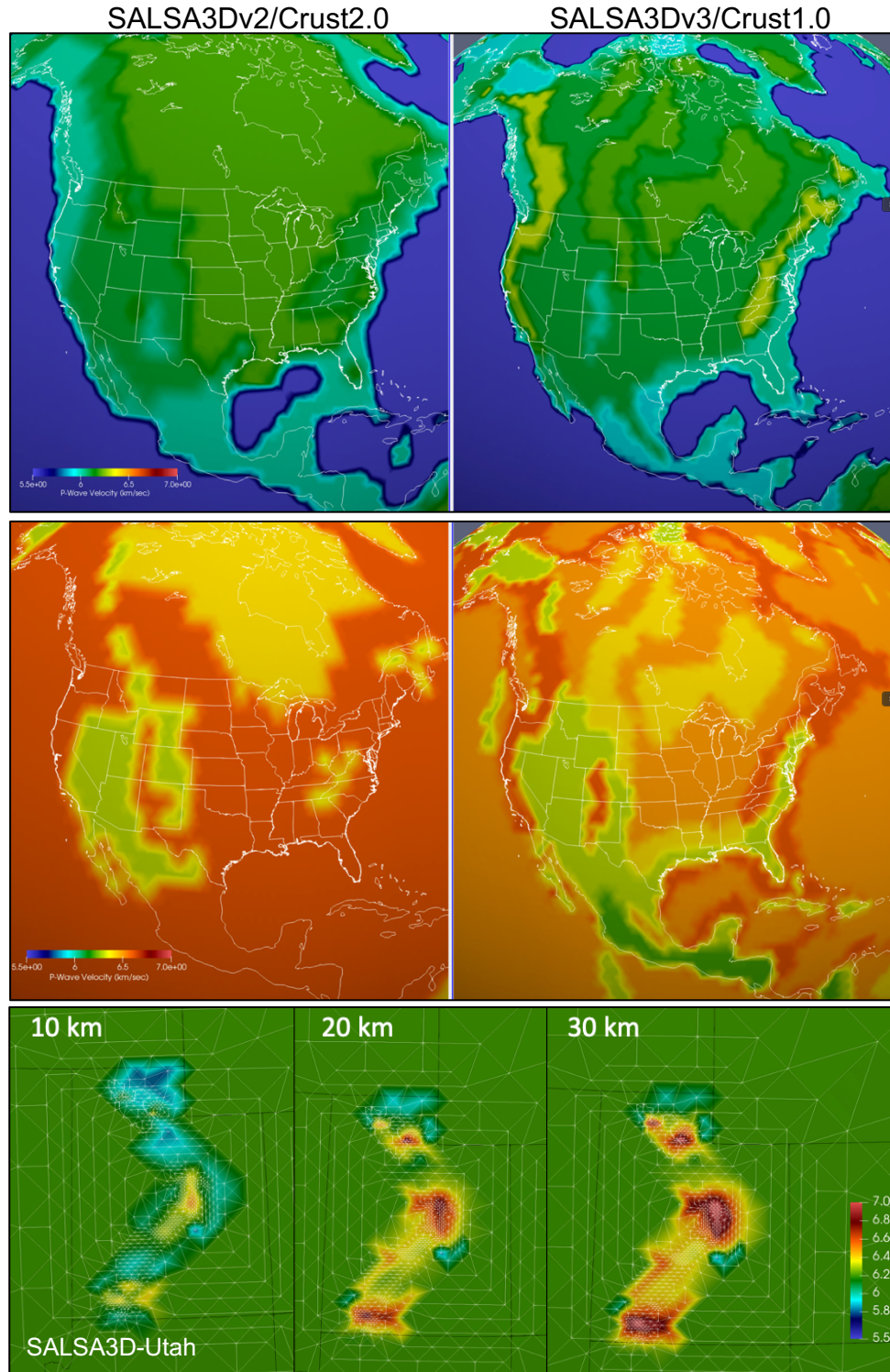


Figure 1. Velocity models for the crust. Top: Upper-crust P-wave velocity in the SALSA3Dv2 (left) and SALSA3Dv3 (right) models. Middle: Mid-crust P-wave velocity in the SALSA3Dv2 and SALSA3Dv3 models. Bottom: P-wave velocities at 10, 20, and 30 km depths in the SALSA3D-Utah model.

2.3. Seismicity Depth Model

Local-distance event locations are particularly susceptible to depth uncertainty, and surface events, such as mining explosions, present the additional challenge of incorporating topography as a constraint on location solutions. We utilize a 3D seismicity depth model in LocOO3D to define the allowable depth range for event locations (Figure 2). The minimum allowable depth (maximum elevation) is based on topography from ETOPO1 gridded at ~1 degree resolution. The GeoTess format of the seismicity depth model allows variable spatial resolution, so the upper surface (topography) of the seismicity depth model used here is defined at ~100 m resolution in Utah. The maximum depth is a smooth surface based on historic seismicity and known tectonics.

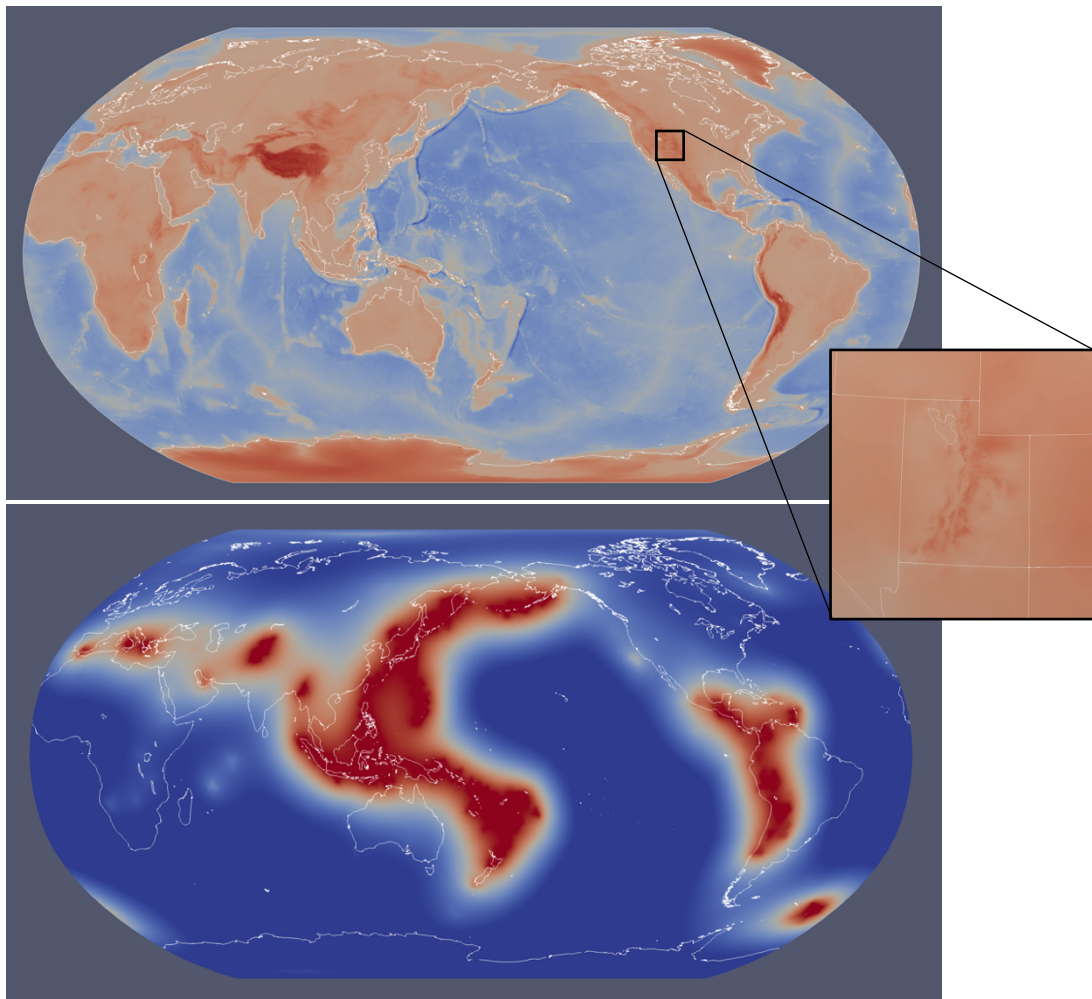


Figure 2. Seismicity Depth Model. Top: Upper limit of the allowable seismicity depth based on topography from ETOPO1. Inset: High-resolution seismicity depth limit based on topography in Utah. Bottom: Lower limit of the allowable seismicity depth based on historic seismic activity and known tectonics.

3. EVENT RELOCATIONS

3.1. Data

3.1.1. UUSS Catalog

The UUSS catalog (Figure 3) is an expanded version of the University of Utah Seismograph Stations (UUSS) network catalog (<https://quake.utah.edu>) that includes quarry blasts and explosions that are typically removed from the published catalog. Events are from mid-2012 to late-2020. Catalog locations are calculated with empirically-determined source- and station-specific 1D velocity profiles. The catalog includes a broad range of well-recorded events from across Utah and into the surrounding states. Data include ~40% local earthquakes with the remainder of the data set comprising quarry blasts and other explosive sources. Phase arrivals are predominantly Pg with ~12% combined Pn, Sg, and Sn arrivals. Data in this catalog also include three well-recorded ground-truth events in the Bingham Mine area with precise source location and timing information.

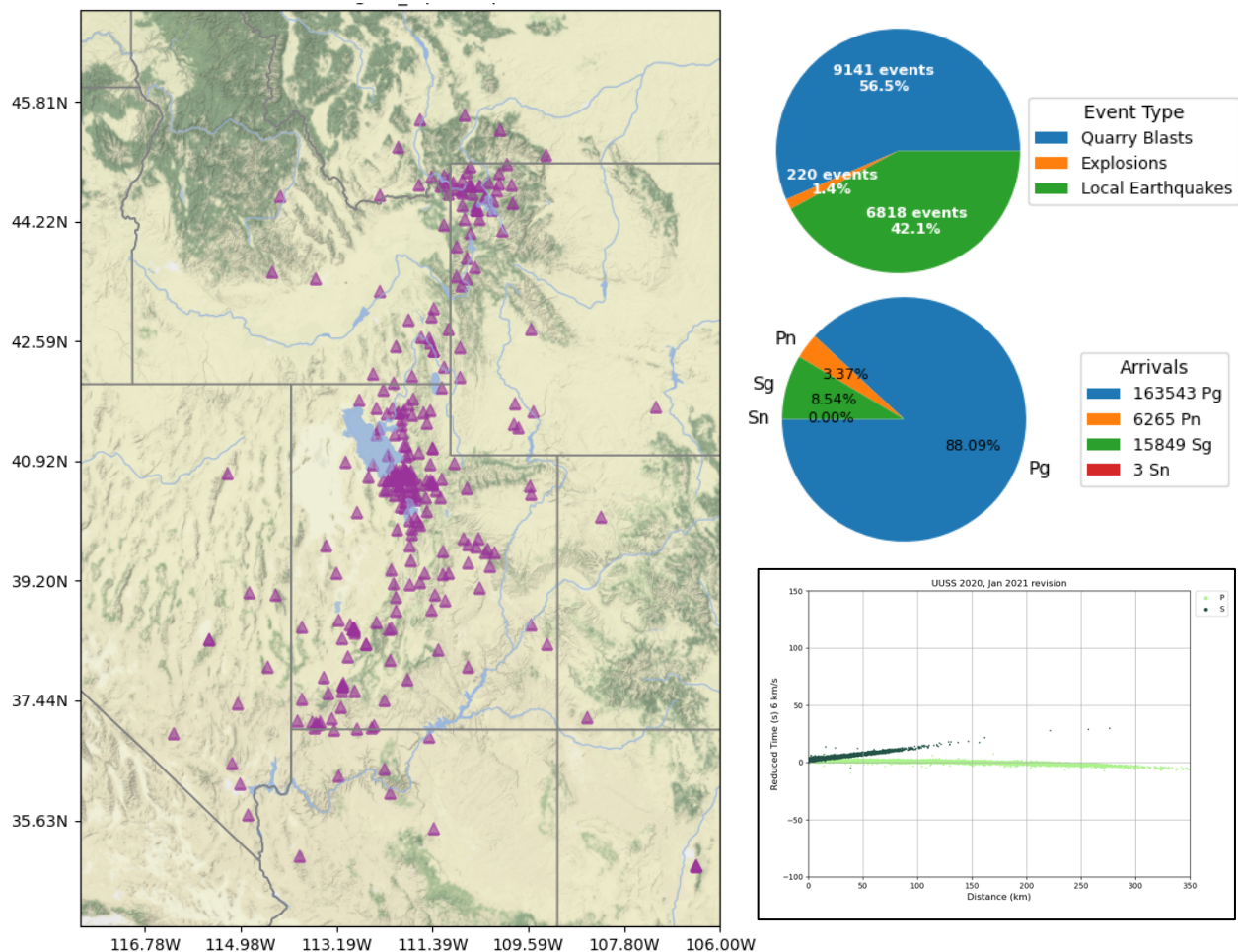


Figure 3. UUSS seismic catalog information. Left: Map showing seismic stations (purple triangles) included in the data in the UUSS catalog. White dot shows location of Bingham Mine ground truth events. Right (top to bottom): Distribution of events based on event type. Distribution of arrivals based on phase identification. Arrival times as a function of distance.

3.1.2. UUEB Catalog

The “UUEB” unconstrained Utah event bulletin catalog (Linville et al., 2019, Figure 4) is an expert-analyst built catalog based on two weeks of data from January 2011. This time window was chosen to include data from local mining districts as well as the mainshock and aftershock sequence from the 3 January, 2011 Circleville, Utah earthquake. The full catalog also includes some regional and teleseismic events recorded during this time window that were removed for this analysis. The expert analyst catalog includes reduced pick errors, smaller magnitude events, and more secondary phases than typical network catalogs. Events include ~75% mining related events, with the remainder being classified as earthquake aftershocks other miscellaneous events. Pg, Pn, Lg, and Sn travel times are used in these relocations.

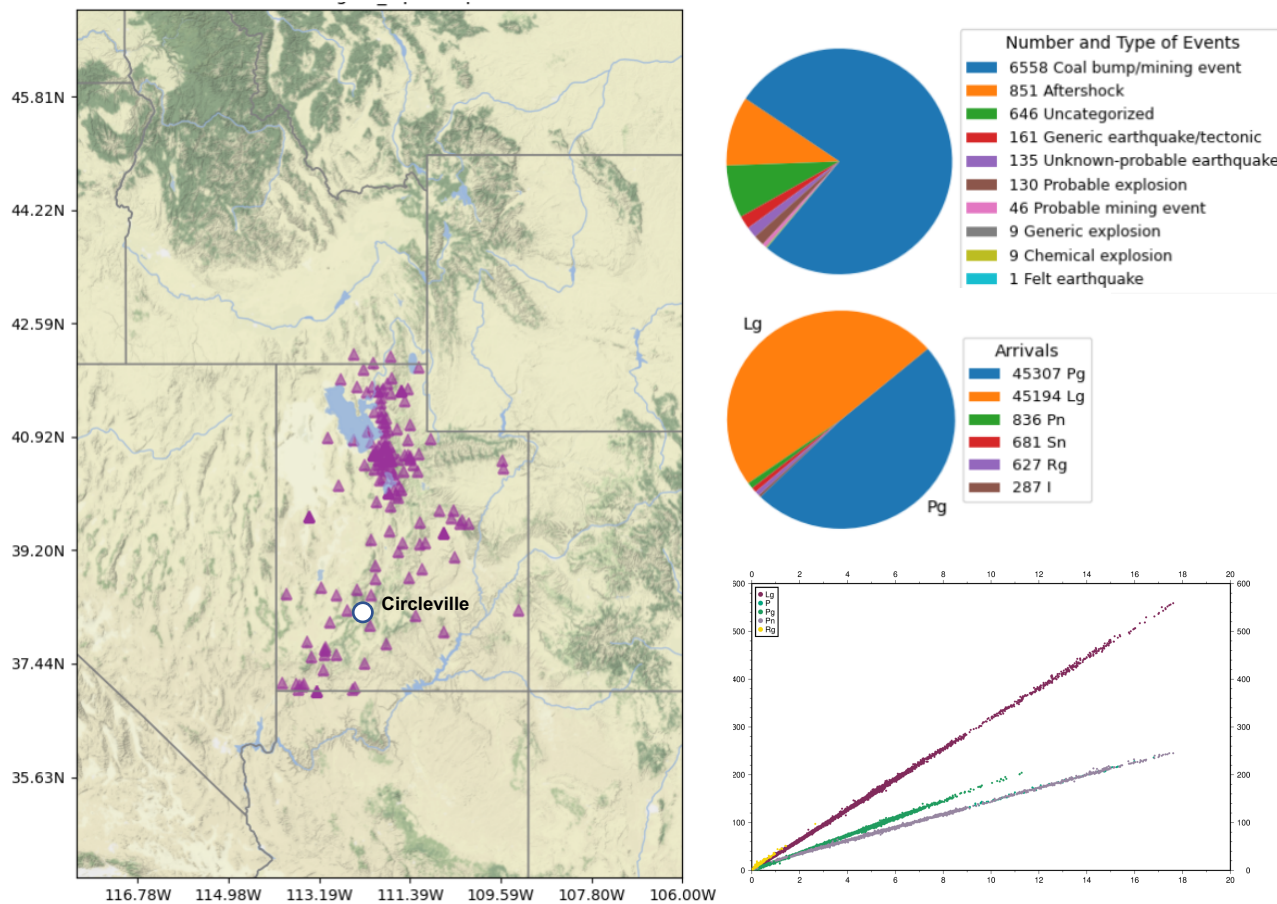


Figure 4. UUEB seismic catalog information. Left: Map showing seismic stations (purple triangles) included in the UUEB catalog data. Right (top to bottom): Distribution of events based on event type. Distribution of arrivals based on phase identification. Arrival times as a function of distance.

3.1.3. Redmond Salt Mine Catalog

The Redmond Mine catalog (Figure 5) is an expert-analyst built catalog based on data recorded from 2017 to 2019 on seismic instruments installed around the Redmond Salt Mine in central Utah. Most arrivals are recorded at < 50 km range and represent signals traveling only through the upper crust from surface events at the mine. Only Pg and Lg phases are considered time defining in these relocations.

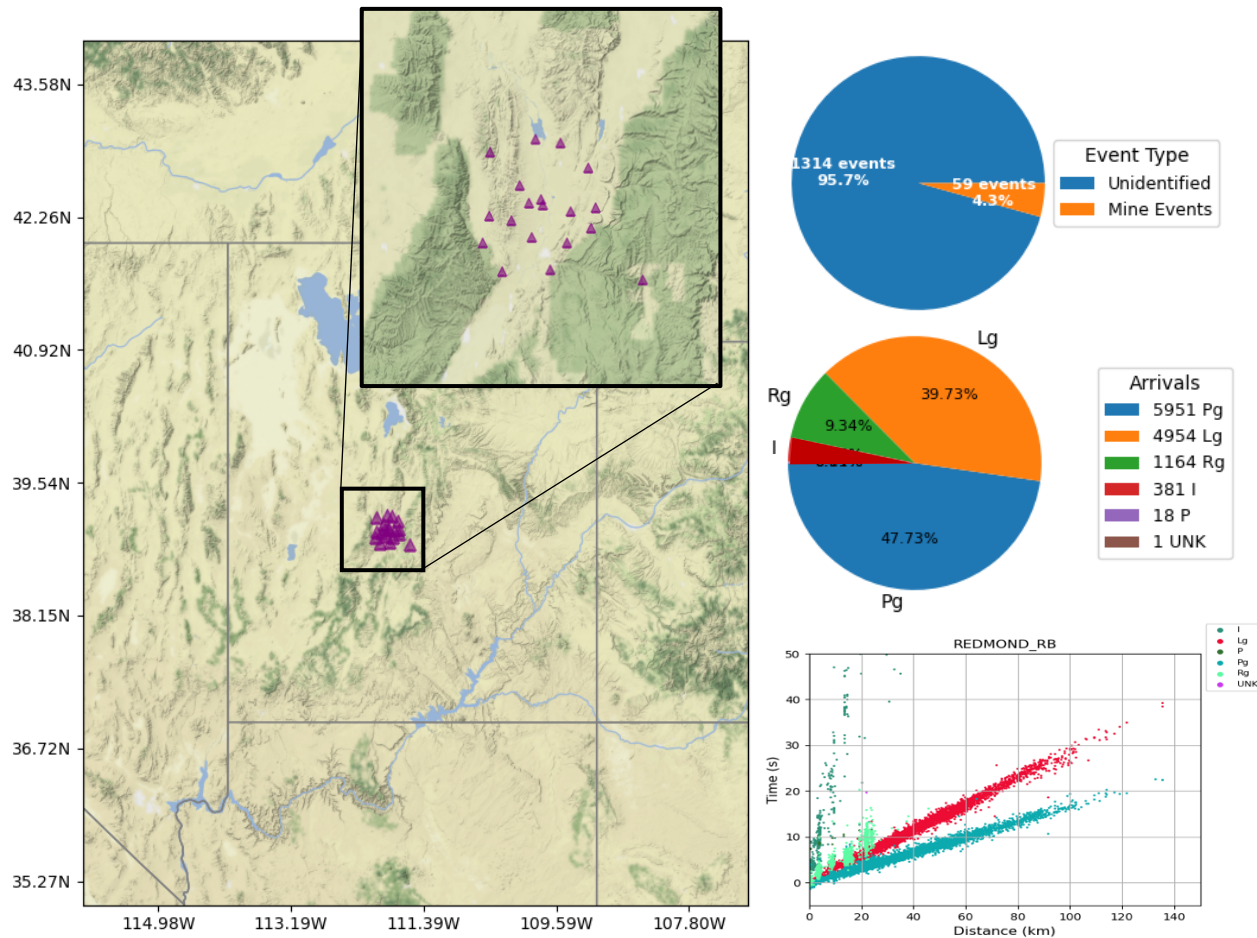


Figure 5. Redmond Salt Mine seismic catalog information. Left: Map showing seismic stations (purple triangles) included in the Redmond catalog data. Right (top to bottom): Distribution of events based on event type. Distribution of arrivals based on phase identification. Arrival times as a function of distance.

3.2. Event Relocations

Events in each catalog were relocated using the velocity models discussed in Section 2, and results were compared to the original catalog locations as well as AK135. Distances between catalog locations and relocated source position are determined as 2D values representing epicentral distance and do not consider changes in event depth. Statistical variations based on the changes in location with each model are indicators of similarity and precision of locations, but do not represent accuracy. The distributions of arrivals for each catalog based on the number of observing stations and maximum azimuthal gap are shown in Figure 6. Events with small numbers of arrivals or large azimuthal gaps are generally less stable when inverting for origin location and time.

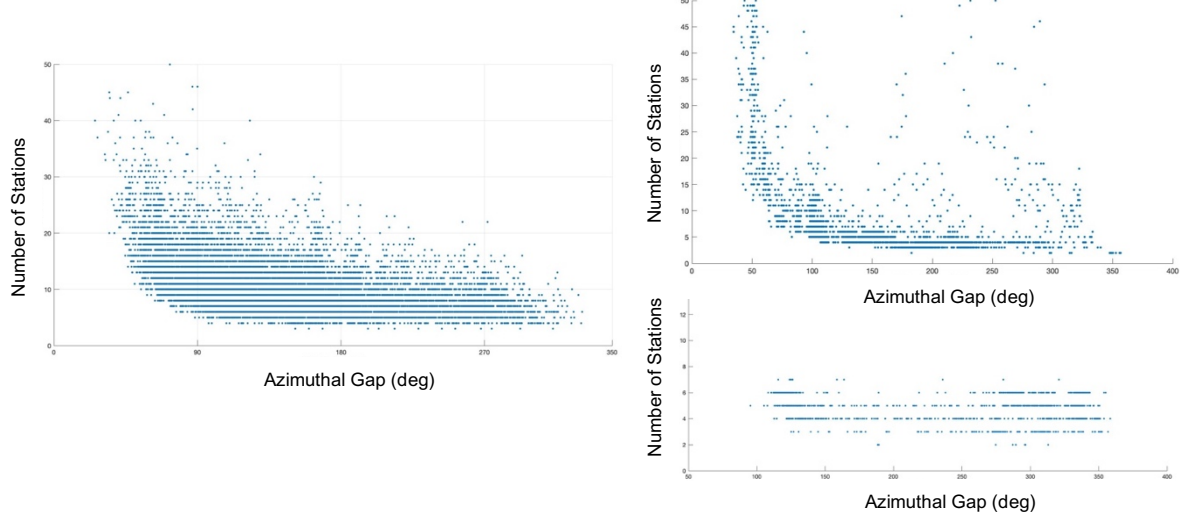


Figure 6. Data distribution for each catalog. Arrivals plotted by number of stations and maximum azimuthal gap. Clockwise from left: UUSS catalog, UUEB catalog, Redmond catalog.

3.2.1. Events from the UUSS Catalog

The UUSS catalog includes ~16,000 mining-related events and earthquake sources located with source- and station-specific 1D velocity profiles. We calculate locations for these events with LocOO3D using the appropriate travel time predictor based on the velocity model type - lookup tables for 1D AK135 and IASP91, the Bender ray tracer for the SALSA3D models, and the RSTT predictor for RSTT. All locations were calculated to the 95% confidence level, and any event that was determined to have fewer arrivals than free parameters (in this case latitude, longitude, depth, and time) was discarded.

The event locations for the UUSS catalog show generally high similarity through central Utah (Figure 7), which includes many of the large mines in the region as well as the epicenter of the Circleville earthquake and aftershock sequence. The mining region in southwest Wyoming shows much higher location variability, which is probably a result of few nearby stations and therefore less robust constraint on event location from near-distance arrivals. When we examine the mean location differences for the UUSS catalog and the AK135 locations, we find that there is notably less variation in the mean distance between locations for different velocity models compared to the UUSS catalog locations. This is likely due to the site-specific 1D velocity profile system used by UUSS effectively approximating 3D model structure at a larger scale. We observe that the number of stations that record an event is a less significant indicator of location stability than the maximum

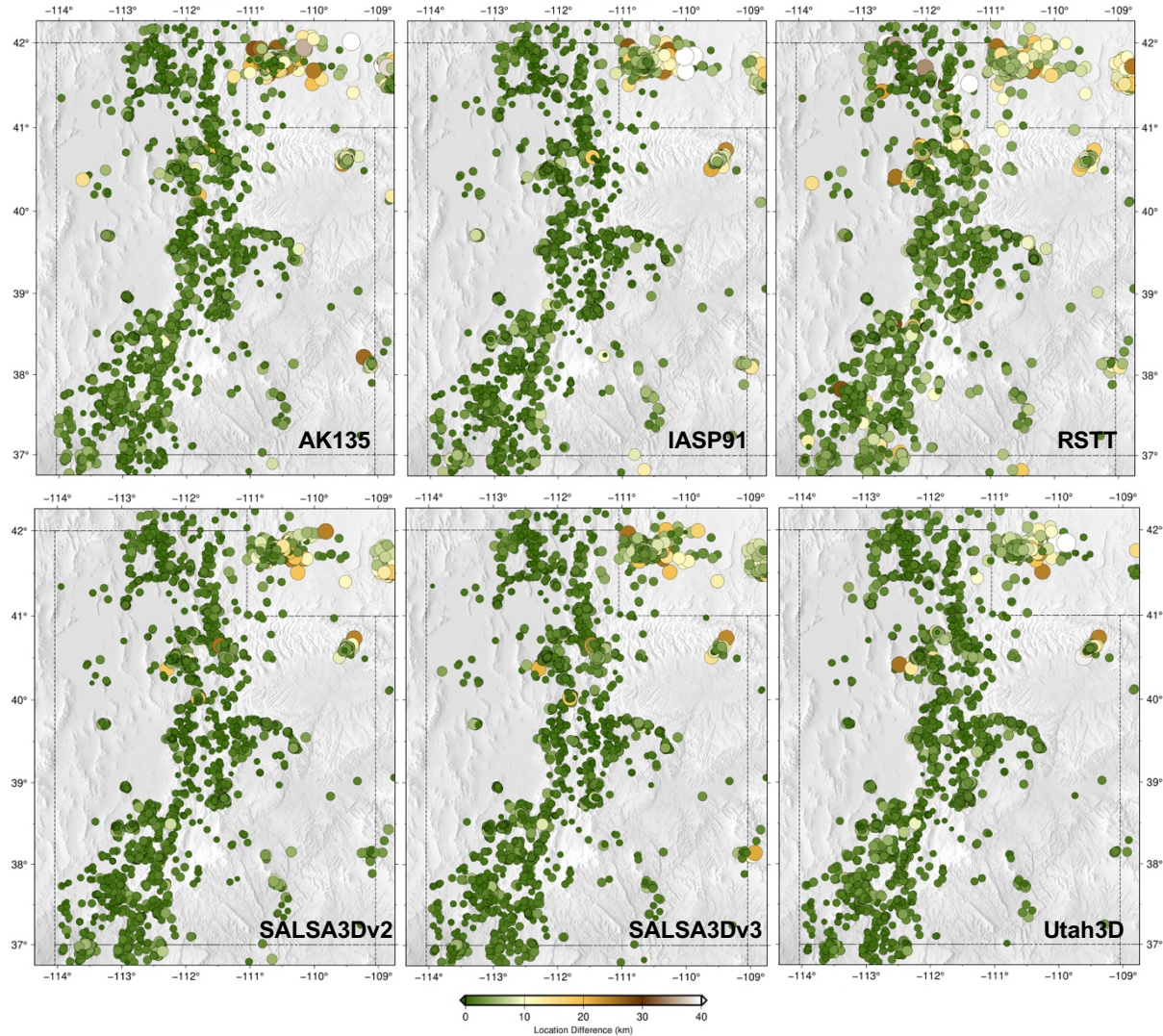


Figure 7. Distance between UUSS Catalog event locations and relocated sources. Based on travel time predictions using velocity models (clockwise from top left) AK135, IASP91, RSTT, Utah3D, SALSA3Dv3, and SALSA3Dv2. Symbol color and size represent distance between catalog origin and relocated source location for each velocity model.

azimuthal gap in station coverage (Figure 8). Events with large azimuthal gaps tend to move significantly greater distances since they have a “path out” direction where the event can move with little or no bounding constraint. This results in much higher uncertainty for these locations, as can be seen in the confidence ellipses for events with a maximum azimuthal gap of <180 degrees and >180 degrees in Figure 9.

LocOO3D performs event relocations based on an initial origin if provided. To explore the influence of the starting location on the final relocation, we also processed the UUSS catalog events through the IASP91, SALSA3Dv2, and SALSA3Dv3 models using locations from AK135 as initial input for LocOO3D. Variability between the resulting locations and those with the UUSS catalog locations as initial input are shown in Figures 10 and 11. A significant majority of events locate within 500 m, however a selection of events locate as much as 30 km apart based on the initial input

location. The events that show poor stability are observed to have large azimuthal gaps, and in most cases the locations are still within the 95% confidence ellipse for both locations.

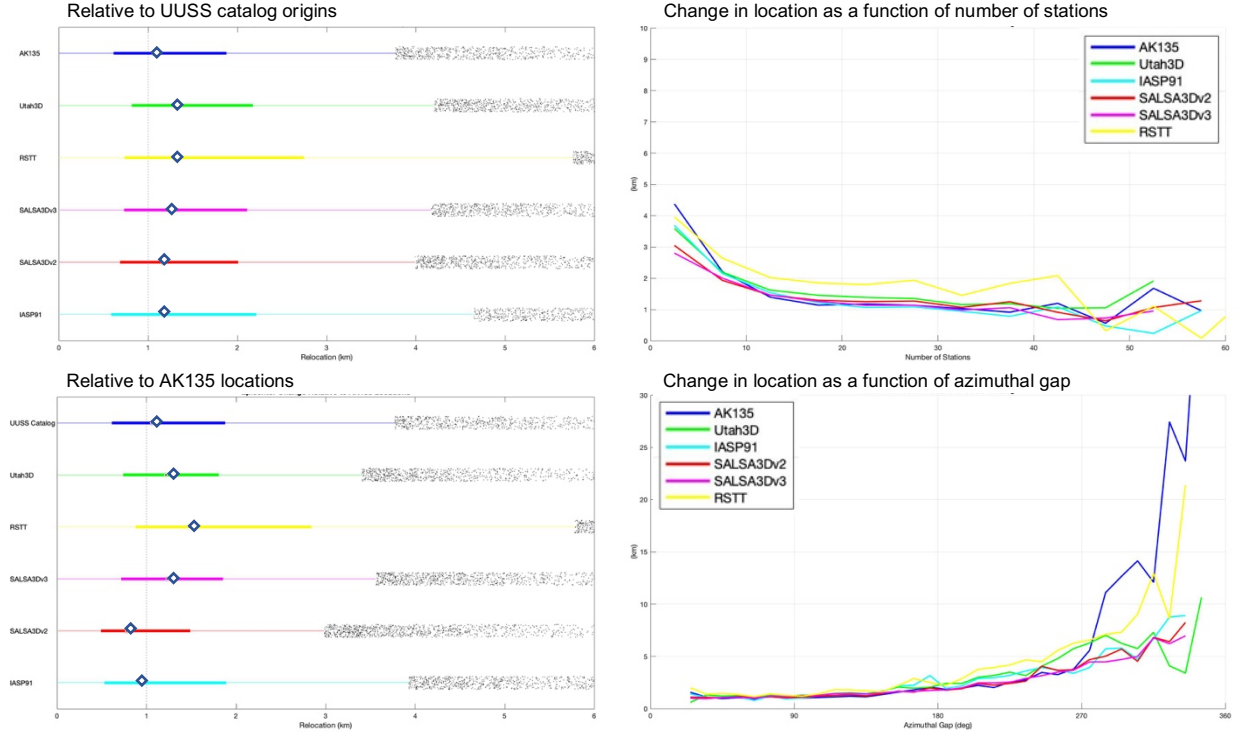


Figure 8. Mean distances between event origins. Left: Mean distances by velocity model. White diamonds represent mean, color bars represent range of 25th and 75th percentiles, black dots represent outliers. Top chart is locations relative to the UUSS catalog locations. Bottom chart is locations relative to AK135 locations. Right: Distance between locations as a function of the number of stations with time-defining arrivals, and distance between locations as a function of azimuthal gap at the origin location.

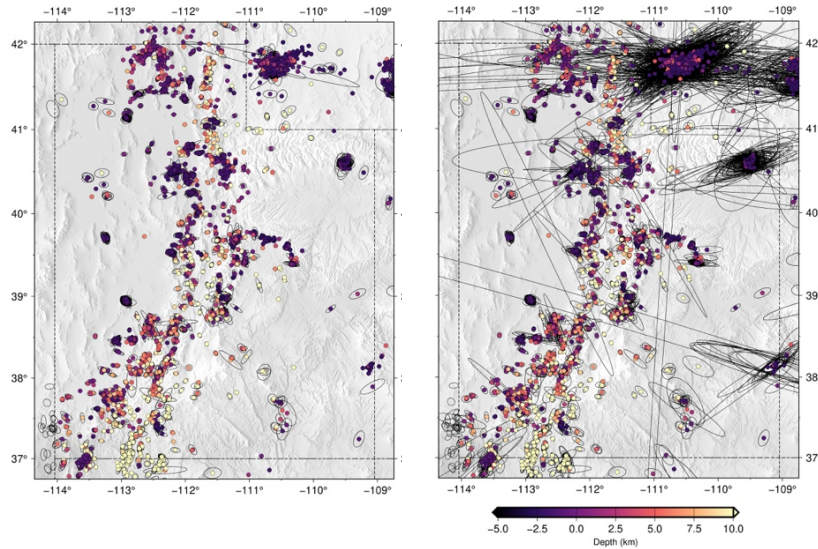


Figure 9. 95% Confidence ellipses based on maximum azimuthal gap. Left: Events with a maximum azimuthal gap < 180 degrees. Right: Events with maximum azimuthal gap > 180 degrees.

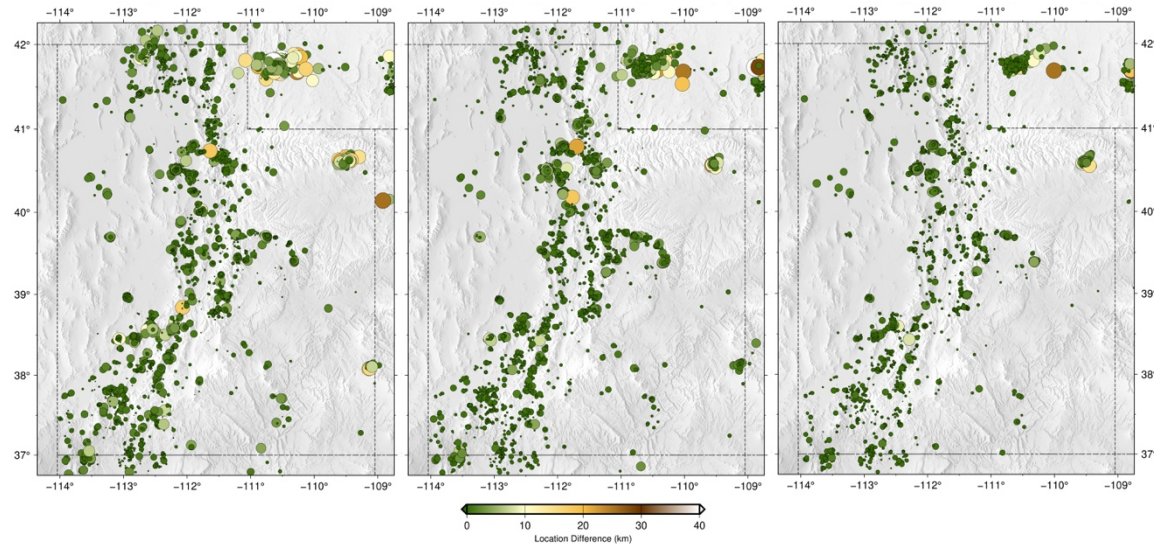


Figure 10. Distance between locations based on initial origins from the UUSS catalog and AK135 locations.

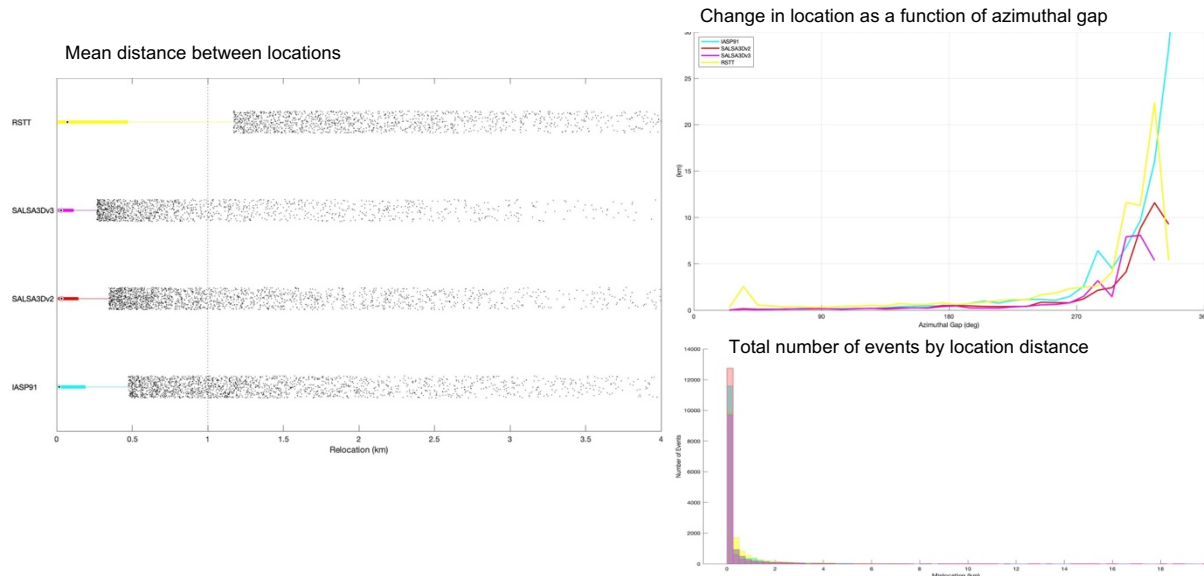


Figure 11. Differences between locations based on initial origin location. Left: Mean distance between locations based on UUSS catalog and AK135 starting origin locations by velocity model. Right: Location differences based on azimuthal gap and total number of location differences.

3.2.2. Events from the UUEB Catalog

The UUEB catalog (Linville et al., 2019) is an expert-analyst built catalog containing ~ 8000 events focused mainly in the mining district in central Utah and in the region of the Circleville earthquake and aftershock sequence in southwest Utah (Figure 12). Additional events are distributed along the Wasatch Front. The mean event relocations for the UUEB catalog reveal greater variability than the UUSS catalog events when compared to both the catalog origins and AK135 locations (Figure 13). Unlike the UUSS catalog, the greatest variability seems to be in central Utah, while the smaller number of events in southwest Wyoming present more stable locations. The greatest difference in event location between the catalog origins and relocated events for the UUEB event locations occurs with the SALSA3Dv3/Crust1.0 model, and this model also produced the largest number of discarded events during relocation ($\sim 50\%$). These factors imply that the structure of Crust1.0 in this

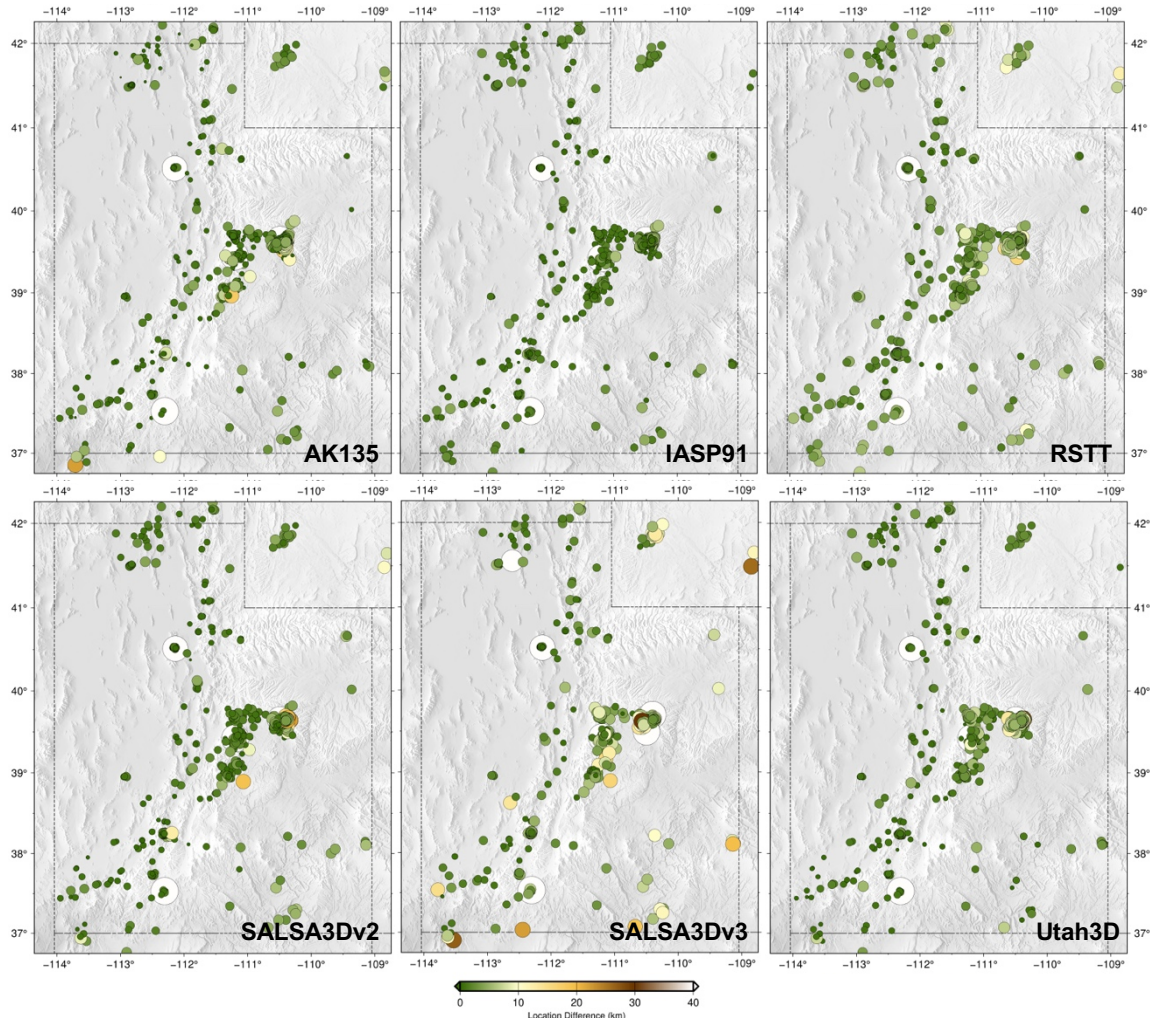


Figure 12. Distance between UUEB Catalog event locations and relocated sources. Based on travel time predictions using velocity models (clockwise from top left) AK135, IASP91, RSTT, Utah3D, SALSA3Dv3, and SALSA3Dv2. Symbol color and size represent distance between catalog origin and relocated source location for each velocity model.

region is not suitable for predicting travel times for the surface-based mining events that dominate this catalog. In contrast, the Utah3D crustal tomographic model produces mostly stable locations, so we can conclude that complex 3D crustal structure alone is not the reason SALSA3Dv3 locations are less satisfactory than other models.

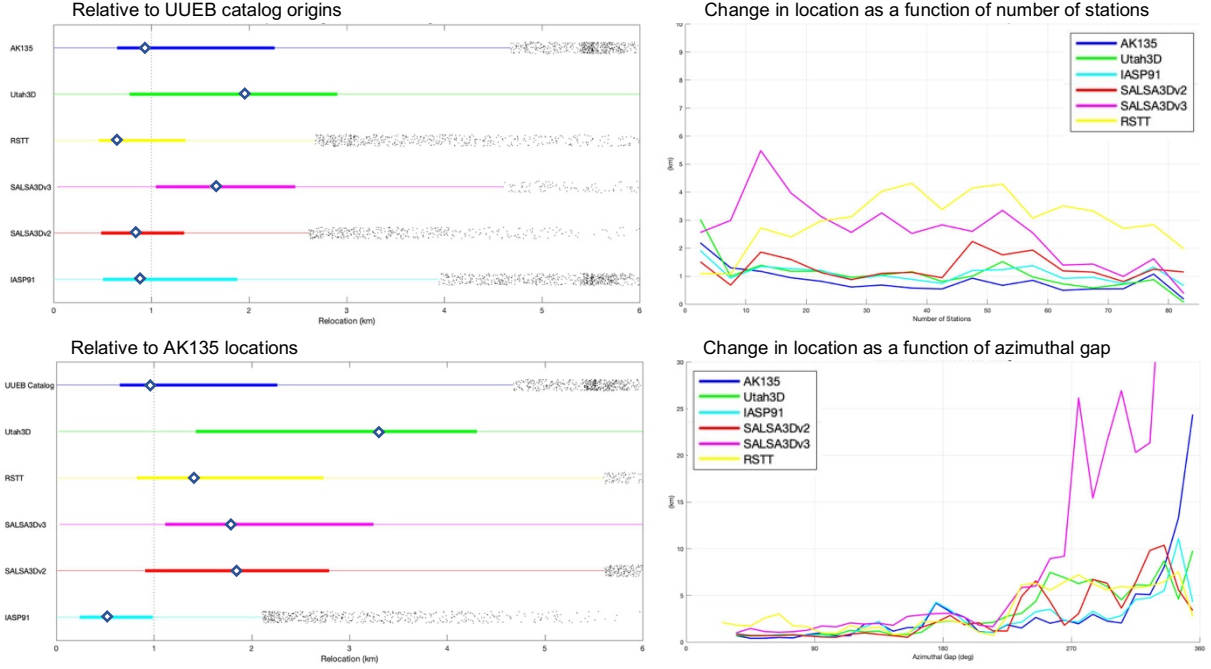


Figure 13. Mean distances between event origins. Left: Mean distances by velocity model. White diamonds represent mean, color bars represent range of 25th and 75th percentiles, black dots represent outliers. Top chart is locations relative to the UUEB catalog locations. Bottom chart is locations relative to AK135 locations. Right: Distance between locations as a function of the number of stations with time-defining arrivals, and distance between locations as a function of azimuthal gap at the origin location.

3.2.3. Events from the Redmond Catalog

The Redmond catalog is an expert-analyst catalog built from data recorded in the area of the Redmond Salt Mine in central Utah (Figure 14). Most arrivals in this catalog are recorded at ranges <50 km from the event, making these locations particularly sensitive to upper crustal velocity structure and local topography. As with the UUEB catalog, we observe the greatest variability in locations using the SALSA3Dv3 model (Figure 15). The SALSA3Dv2 model produces the smallest distribution of location changes, while the Utah3D model resulted in the greatest number of discarded events. Events recorded at these distance ranges tend to be inherently unstable in depth, even when there is good azimuthal coverage, due to the relative travel time errors imposed over short path distances from imperfect velocity models. Locations for events at very local distances like these are improved by including shallow crustal velocity layers and restricting anthropogenic events to depths equivalent to a high-resolution topographic surface.

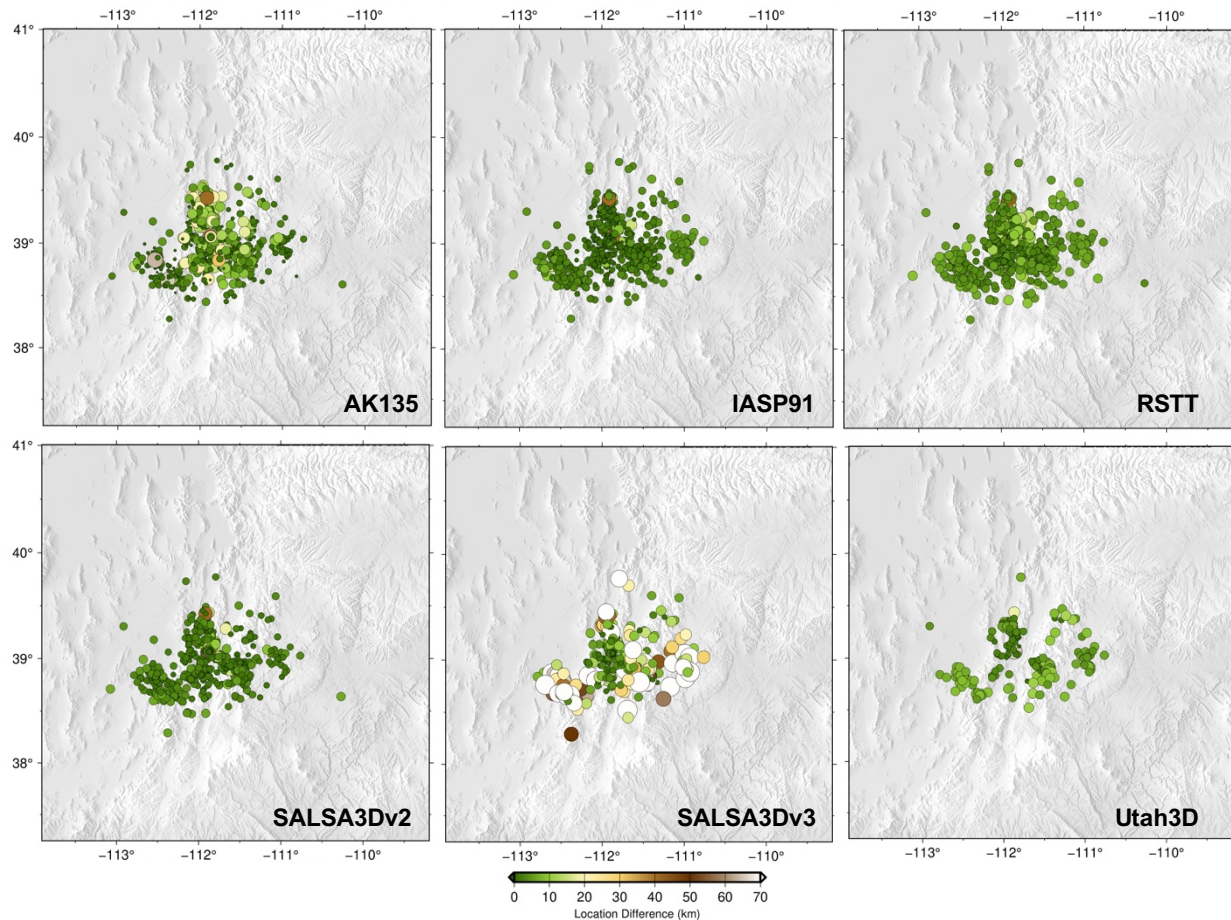


Figure 14. Distance between Redmond Catalog event locations and relocated sources. Based on travel time predictions using velocity models (clockwise from top left) AK135, IASP91, RSTT, Utah3D, SALSA3Dv3, and SALSA3Dv2. Symbol color and size represent distance between catalog origin and relocated source location for each velocity model.

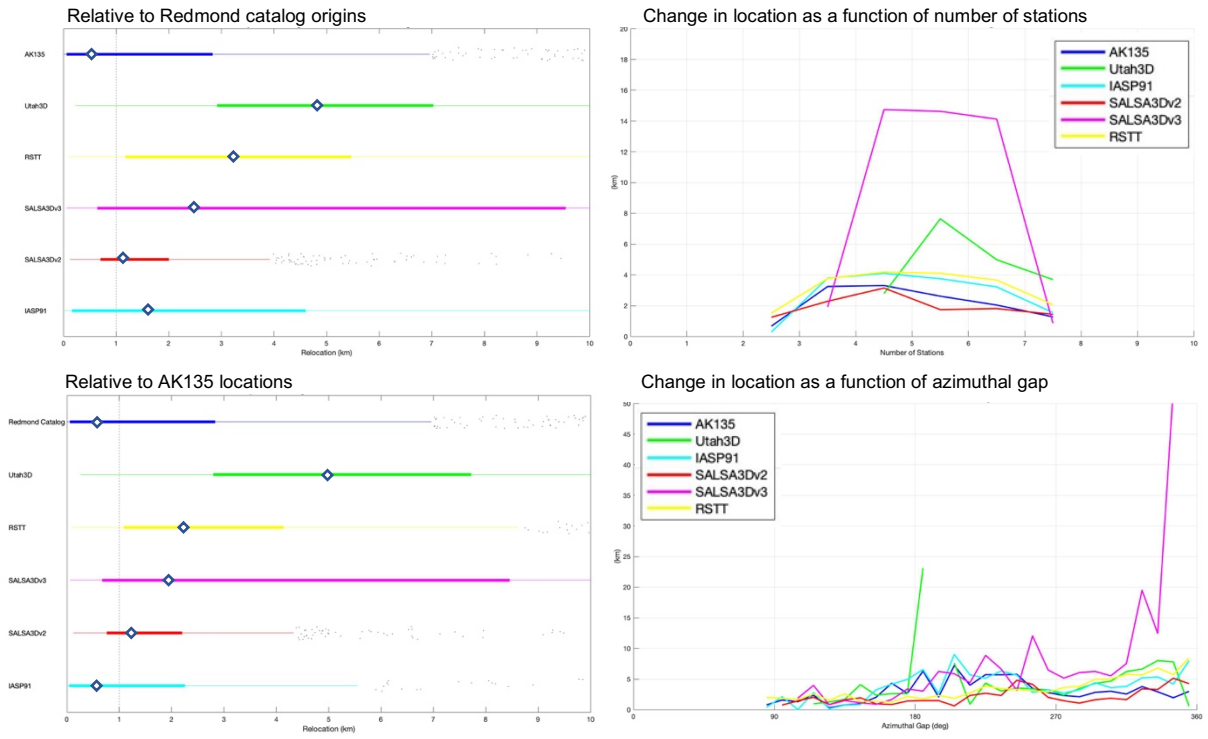


Figure 15. Mean distances between event origins. Left: Mean distances by velocity model. White diamonds represent mean, color bars represent range of 25th and 75th percentiles, black dots represent outliers. Top chart is locations relative to the Redmond catalog locations. Bottom chart is locations relative to AK135 locations. Right: Distance between locations as a function of the number of stations with time-defining arrivals, and distance between locations as a function of azimuthal gap at the origin location.

This page left blank.

4. SUMMARY

As the seismic monitoring community advances toward locating and characterizing ever-smaller events, the need is constantly increasing for higher resolution, higher fidelity data and models for determining event locations and accurately assessing confidence in those locations. Local-distance seismic data are a crucial element for analyzing small events and understanding the complexities of locating events with crustal seismic phases. Using Utah as a test case, we examined three data sets of varying duration, finesse, and magnitude to compare the effects of local velocity models, topography, and input parameters on location stability. We determine that the most critical elements controlling relocation precision are azimuthal coverage and local velocity structure, with tradeoffs between the two based on event depth, type, location, and range.

Ongoing improvements to the accuracy and precision of local-distance seismic event locations depend on:

- Sufficient data coverage
- Accurate arrival picks and phase identification
- Versatile location algorithm
- Sufficient earth information
- High fidelity travel-time predictions
- Robust uncertainty estimates

and could also include:

- High resolution 3D crustal velocity models
- Improved ray tracing approximations for crustal phases (particularly Pg, Pn)
- Incorporating full waveform information in location estimates
- Incorporating infrasound information in location estimates

Focusing on these elements will allow us to continue improving event location reliability and accuracy across the range of distance scales including local, regional, and global events.

REFERENCES

- [1] Anderson, J., Farrell, W. E., Garcia, K., Given, J., & Swanger, H. (1990). Center for seismic studies version 3 database: Schema reference manual. *CSS Technical Report C90-01*.
- [2] Ballard, S., Hipp, J., Kraus, B., Encarnacao, A., Young, C. (2016). GeoTess: A Generalized Earth Model Software Utility. *Seismological Research Letters* 87 (3), 719–725.
- [3] Ballard, S., J. R. Hipp, M. L. Begnaud, C.J. Young, A. V. Encarnacao, E. P. Chael and W. S. Phillips (2016b) SALSA3D: A tomographic model of compressional wave slowness in the Earth's mantle for improved travel-time prediction and travel-time prediction uncertainty. *Bulletin of the Seismological Society of America* **106** (6), 2900-2916.
- [4] Ballard, S., Hipp, J., Young, C. (2009). Efficient and Accurate Calculation of Ray Theory Seismic Travel Time through Variable Resolution 3D Earth Models. *Seismological Research Letters* 80 (6), 989–999.
- [5] Bassin, C., Laske, G. and Masters, G., (2000). The Current Limits of Resolution for Surface Wave Tomography in North America, EOS Trans AGU, 81, F897.
- [6] Geiger, L. (1910), Herdbestimmung bei erdboden ans den ankunftzeiten, K. Gessel. Wiss. Goett. v. 4, pp. 331-349.
- [7] Jordan, T. H. and K. A. Sverdrup (1981), Teleseismic Location Techniques and their Application to Earthquake Clusters in the South-Central Pacific, *Bull. Seis. Soc. Am.*, v. 71.
- [8] Kennett, B.L.N. (Compiler and Editor). (1991). IASPEI 1991 Seismological Tables. *Bibliotech*, Canberra, Australia, 167 pp.
- [9] Kennett, B.L.N. Engdahl, E.R. & Buland R., (1995). Constraints on seismic velocities in the Earth from travel times, *Geophys J Int*, **122**, 108-124.
- [10] Lay, T., and T. C. Wallace (1995), *Modern Global Seismology*, Academic Press.
- [11] Levenberg, K. (1944), A method for the solution of certain non-linear problems in least squares, *Quart. Appl. Math.*, v. 2, pp. 164-168.
- [12] Laske, G., Masters., G., Ma, Z. and Pasyanos, M., (2013). Update on CRUST1.0 - A 1-degree Global Model of Earth's Crust, *Geophys. Res. Abstracts*, 15, Abstract EGU2013-2658.
- [13] Linville, L., Brogan, R. C., Young, C., & Aur, K. A. (2019). Global- and Local-Scale High-Resolution Event Catalogs for Algorithm Testing. *Seismological Research Letters* 90.
- [14] Marquardt, D. W. (1963), Journal of the Society for Industrial and Applied Mathematics, v. 11, pp. 431-441.
- [15] Phillips, W. S., M. L. Begnaud, C. A. Rowe, L. K. Steck, S. C. Myers, M. E. Pasyanos, and S. Ballard (2007). Accounting for lateral variations of the upper mantle gradient in Pn tomography studies. *Geophys. Res. Lett.*, **34**(14). 5 pp.
- [16] Press, W. H., S. A. Teukolsky, W. T. Vetterling, and B. P. Flannery (2002). *Numerical Recipes in C++: The Art of Scientific Computing*. 2nd ed. New York: Cambridge University Press.
- [17] Um, J., and C. H. Thurber (1987). A fast algorithm for two-point seismic ray tracing. *Bulletin of the Seismological Society of America* 77, 972–986.
- [18] Zhao, D., A. Hasegawa, and S. Horiuchi (1992). Tomographic imaging of P and S wave velocity structure beneath northwestern Japan. *Journal of Geophysical Research* 97 (B13), 19,909–19,928.

DISTRIBUTION

Email—Internal

Name	Org.	Sandia Email Address
Christopher Young	06371	cjyoung@sandia.gov
Kathy Davenport	06756	kdavenp@sandia.gov
Stephanie Teich-McGoldrick	06756	steichm@sandia.gov
Technical Library	01977	sanddocs@sandia.gov

This page left blank.

This page left blank

This page left blank



**Sandia
National
Laboratories**

Sandia National Laboratories is a multimission laboratory managed and operated by National Technology & Engineering Solutions of Sandia LLC, a wholly owned subsidiary of Honeywell International Inc. for the U.S. Department of Energy's National Nuclear Security Administration under contract DE-NA0003525.